DOI:10.16555/j.1006-8775.2015.02.001

Article ID: 1006-8775(2015) 02-0101-10

AN OPERATIONAL STATISTICAL SCHEME FOR TROPICAL CYCLONE INDUCED RAINFALL FORECAST

LI Qing-lan (李晴岚)[1], LAN Hong-ping (兰红平)[2], Johnny C L CHAN (陈仲良)[3], CAO Chun-yan (曹春燕)[2], LI Cheng (李 程) [2], WANG Xing-bao (王兴宝)[1, 4]

(1.Shenzhen Institute of Advanced Technology, Chinese Academy of Sciences, Shenzhen 518055 China; 2. Shenzhen Meteorological Bureau, Shenzhen 518040 China; 3. Laboratory for Atmospheric Research, Department of Physics and Materials Science, City University of Hong Kong, Hong Kong, China; 4. Centre for Australian Weather and Climate Research, Bureau of Meteorology, Melbourne VIC 3001 Australia)

Abstract: A non-parametric method is used in this study to analyze and predict short-term rainfall due to tropical cyclones (TCs) in a coastal meteorological station. All 427 TCs during 1953-2011 which made landfall along the Southeast China coast with a distance less than 700 km to a certain meteorological station - Shenzhen are analyzed and grouped according to their landfalling direction, distance and intensity. The corresponding daily rainfall records at Shenzhen Meteorological Station (SMS) during TCs landfalling period (a couple of days before and after TC landfall) are collected. The maximum daily rainfall (R-24) and maximum 3-day accumulative rainfall (R-72) records at SMS for each TC category are analyzed by a non-parametric statistical method, percentile estimation. The results are plotted by statistical boxplots, expressing in probability of precipitation. The performance of the statistical boxplots is evaluated to forecast the short-term rainfall at SMS during the TC seasons in 2012 and 2013. Results show that the boxplot scheme can be used as a valuable reference to predict the short-term rainfall at SMS due to TCs landfalling along the Southeast China coast.

Key words: tropical cyclone; rainfall forecast; non-parametric method; boxplot

CLC number: P444 **Document code:** A

1 INTRODUCTION

Tropical cyclones (TCs) are among the most destructive natural phenomena. TCs often bring about strong wind, heavy rainfall and storm surge to the area along or close to their track. Among the three effects, heavy rainfall, which may lead to flash flooding and mudslides, is the most lethal natural disaster (Willoughby et al. [1]). Interacting with a strong southwest monsoon, Typhoon Morakot produced copious amounts of rainfall in the island of Taiwan, with a record of 3 031.5 mm during August 6-13, 2009 (Wu et al.[2]). Hurricane Katrina, one of the deadliest hurricanes in the history of the United States, brought over 15 inches (381 mm) of heavy rainfall to Florida at its landfall. The recorded maximum sustained wind speed reached 175 mph (280 km/h) and wind gusts reached 220 mph (350 km/h) at New Orleans, Louisiana (Jonkman et al.[3]). Typhoon Morakot left 619 people dead and the death toll due to hurricane Katrina was over 1 100 (Jonkman et al.[3]; Cui et al.[4]; Knabb et al.[5]). In order to alleviate enormous loss of lives and properties in the future, it is important to notify the local population and civil authorities to make appropriate preparation for the cyclones, including evacuation of the vulnerable areas where necessary. Accurate and timely (24 h and 12 h before landfall) forecasting the TC track and the potential rainfall and wind induced by TC is vital and essential (Kidder et al.[6]).

Most operational meteorologists rely heavily on numerical weather prediction (NWP) models in forecasting TCs. TC track forecasts have improved significantly over the past several decades (Willoughby et al.[1]; Aberson [7]; Fei et al.[8]; Rogers et al.[9]). By contrast, the improvement in forecasting the TCs intensity has lagged behind the progress of TCs track forecasting (Rogers et al.[9]; DeMaria and Gross[10]; Cecil et al.[11]; Knaff et al.[12]). The capability for NWP models to predict short-term rainfall is still very limited (Willoughby et al.[1]; Kidder et al. [6]; Marchok et al. [13]; Liu et al. [14]). Quantitative forecasting of rainfall remains problematic and lags behind the TCs track forecast, although TC forecasting is a successful enterprise with favorable benefit-to-cost returns[1]). Kidder et al.[6] reported that because few observations are available while the storm is offshore, initializing numerical weather prediction models with sufficient details of the storm is impossible. Therefore, the rainfall forecasts by NWP models are not so accurate.

Received 2014–07–02; **Revised** 2015–02–02; **Accepted** 2015–04–15

Foundation item: The Innovation of Science and Technology Commission of Shenzhen Municipality (JCYJ20120617115926138); Scientific and Technological Project for Regional Meteorological Center in South China, Chinese Meteorological Administration (GRMC2012M15)

Biography: LI Qing–lan, associate professor, primarily undertaking research on climate change and weather forecasting.

Corresponding author: LI Qing–lan, e–mail: ql.li@siat.ac.cn

The research of Xu et al.[15] shows that currently in China, there is no effective operational approach to forecast the heavy rainfall and wind induced by TCs. The forecast of the rainfall and wind due to TCs in China all relies on NWP models and the experience of forecasters. Exploring other ways to predict short-term rainfall is therefore important and necessary.

When TCs approach the land or move across the coast, the TCs structure and intensity change greatly (Chen[16]). Landfalling TCs usually bring about heavy rainfall over land. Regarding the forecasting of rainfall due to a TC in a certain region (at a certain rain gauge), it is reported that the rainfall is associated with the distance from the TC center, TC intensity, TC track, TC moving velocity and TC residing time, as well as the environmental background. Rainfall induced by a TC generally decreases exponentially with distance from the TC center (Kidder et al.[6]; Simpson and Riehl[17]; Pfost[18]). With the same environmental background, the stronger the TC intensity, the heavier the precipitation will be[18]. The distribution of precipitation due to landfalling TC is asymmetric. In the Northern Hemisphere, the land on the right hand side of TC would usually receive more intense and widespread rainfall than the land on the left hand side (Chan and Liang[19]), since the rain bands on the right would carry more moist oceanic air than those on the left. After landfall, the slower the moving speed of the TC or the longer the residence time for the TC in a certain region, the more opportunities and longer time will be for the TC to interact with other weather systems, which might lead to extreme rainfall accumulation[2].

The previous studies indicate that rainfall induced by a TC at a certain rain gauge is attributable to a variety of factors. However, most of those studies focused on either case studies or on investigating a specific factor and the conclusion is mostly qualitative. In this study, we will develop a statistical scheme to forecast the maximum daily rainfall and three-day accumulative rainfall at a meteorological station by considering the factor of distance between the station and the TC landfalling center, the intensity of the TC and the landfalling direction of the TC. This paper is arranged as follows. An overview of the data and methodology is presented in section 2. Section 3 contains the description of the statistical boxplot scheme for TCs rainfall. The applications of the boxplot scheme to forecast the rainfall due to TCs in 2012 and 2013 are described in section 4. Summaries and conclusions are given in the final section.

2 DATA AND METHODOLOGY

This study focuses on Shenzhen to explore the potential rainfall caused by landfalling TCs. Shenzhen is a coastal and urban city in Guangdong Province, China (Wang et al.[20]; Zhang et al.[21]; Chen et al.[22]; Li and Chen [23]), with the latitude from 22°27' to 22°52' and longitude from 113°46' to 114°37' (Fig.1). In summer and autumn, the city is often influenced by TCs. In this study, a total of 427 TCs, which made landfall along the Southeast China coast from 1953 to 2011 with the landfalling distance within 700 kilometers to Shenzhen meteorological station (SMS), are studied.

The records of daily rainfall from 1953 to 2011 in SMS are obtained from Shenzhen Meteorological Bureau (SZMB). The maximum daily rainfall (from 20:00 (Beijing Time, or BT, the same below) of the previous day to 20:00 BT of the current day) and the maximum three-day accumulative rainfall at SMS during the TC landfalling period (within a couple of days before or af-

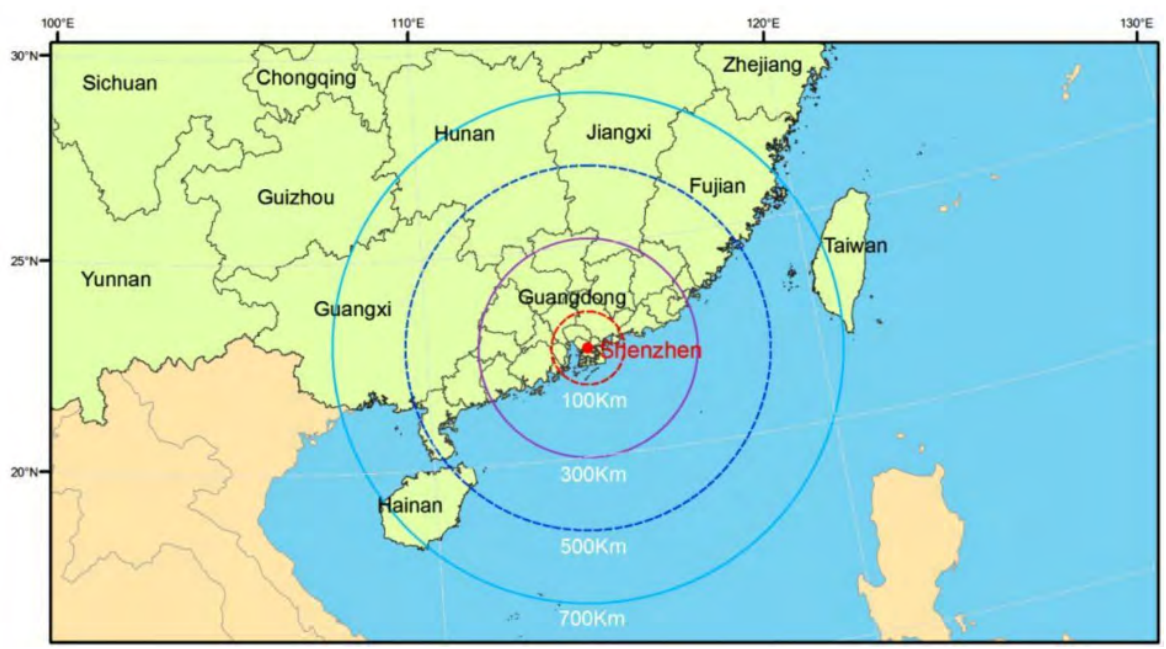

Figure 1. Location of SMS. Circles indicate regions with radii of 100, 300, 500, 700 km to SMS.

Table 1. TC intensity scale according to CMA.

Category	Abbreviation	Sustained max winds near the eye
Super Typhoon	SuTY	⩾51 m/s
Severe Typhoon	STY	41.5 to 50.9 m/s
Typhoon	TY	32.7 to 41.4 m/s
Severe Tropical Storm	STS	24.5 to 32.6 m/s
Tropical Storm	TS	17.2 to 24.4 m/s
Tropical Depression	TD	10.8 to 17.1 m/s

ter landfall) are computed. For example, if a TC makes landfall on date A, the rainfall at SMS on date A-2, A-1, A, A+1, A+2 is collected as R_{A-2}, R_{A-1}, R_A, R_{A+1}, R_{A+2}. The maximum daily rainfall (R-24) and the maximum three-day accumulative rainfall (R-72) are computed as follows:

$$R\text{-}24=\max(R_{A-2},R_{A-1},R_A,R_{A+1},R_{A+2}) \quad (1)$$

$$R\text{-}72=\max(R_{A-2}R_{A-1}R_A,\ R_{A-1}R_AR_{A+1},\ R_AR_{A+1}R_{A+2}) \quad (2)$$

where $R_{A-2}R_{A-1}R_A$ refers to the accumulative rainfall on date A-2, A-1, A, etc.

TC characteristics from 1953 to 2011 are collected from China Meteorological Administration (CMA). The TC characteristics include the landfalling track, the distance between the TC landfalling center and SMS, and the intensity (maximum wind speed near the TC center), which are proved to be strongly related to the rainfall caused by TCs in a certain region[6, 17-19].

As the rainfall distribution and intensity on the right side of TC track is different from those on the left side of TC track [19], all the TCs are first grouped into two main categories: Category A: TCs landfalling to the west of SMS (landfalling longitude < 114°E) and Category B: TCs landfalling to the east of SMS (landfalling longitude > 114°E). Next, A and B are further grouped into 7 categories according to the landfalling distance to SMS, e.g. A1, within 100 km; A2, 100-200 km; A3, 200-300 km; … A7, 600-700 km and B1, within 100 km; … B7, 600-700 km. Finally, A1, A2 … B7 are grouped according to their landfalling intensity. According to the typhoon categorizing criterion of CMA (Table 1), there are six categories of TCs, which are super typhoon, severe typhoon, typhoon, severe tropical storm, tropical storm and tropical depression. Among the 427 TCs, no landfalling TC was super typhoon. In this study, we classify the TC intensity into three categories based on their respective TC landfalling intensity scale (Table 1): TTY (total typhoon), which includes SuTY, STY and TY; TTS (total tropical storm), which includes STS, TS; and TD. A1, A2, …, B7 are therefore grouped into A1-TTY, A1-TTS, A1-TD, A2-TTY, A2-TTS, A2-TD, … , B7-TTY, B7-TTS, and B7-TD. The flowchart of the TCs' categorizing steps is depicted in Fig.2.

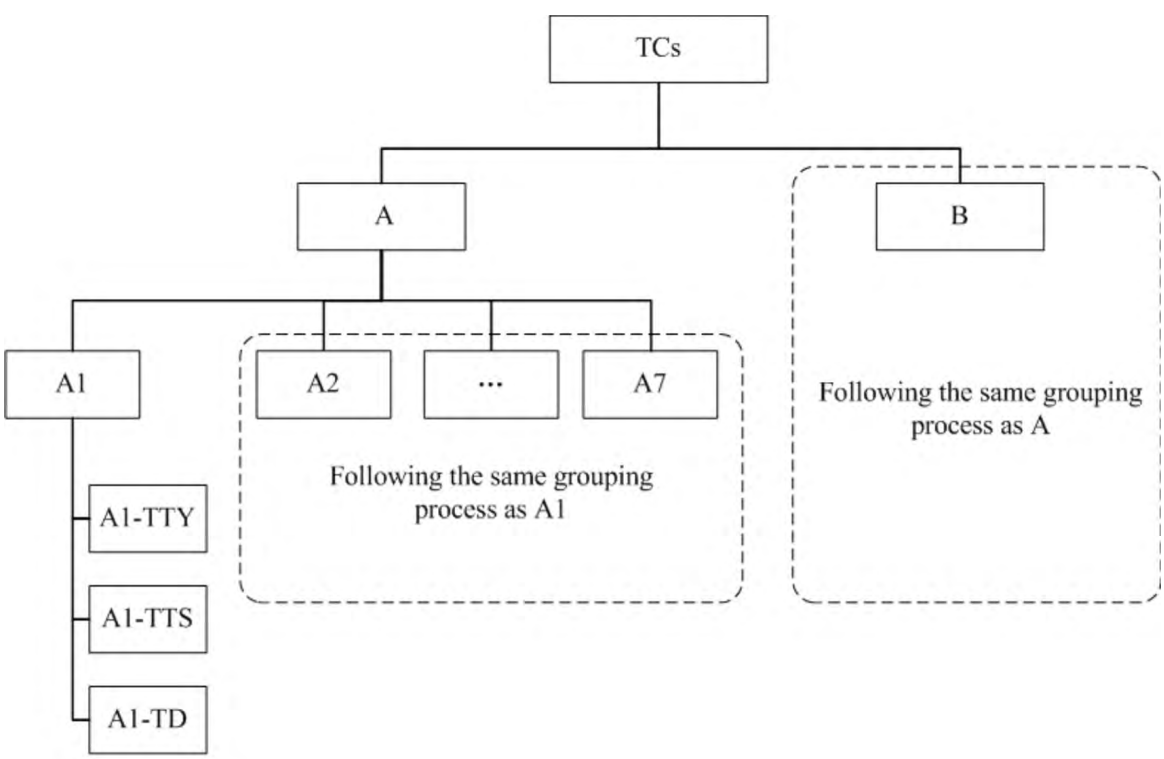

Figure 2. Flowchart of grouping process for landfalling TCs along the Southeast China coast.

Due to its nature of abnormal distribution for precipitation (Turco and Llasat [24]), a non-parametric method is a more preferable approach to analyze typhoon-induced precipitation than a parametric method (Pett [25]). The non-parametric statistical method, percentile estimation, is used to analyze the rainfall data in this study. Boxplots are applied to illustrate the analysis results. The detailed procedures are as follows:

Given n sorted rainfall observation $\{r_i\}$, i=1, ⋯, n, for a TC category, $0 < r_1 < r_2 < \cdots < r_n$, the corresponding percentile for a rainfall record, r_i , is computed to be (Stark and Woods[26]):

$$P_i = \frac{100}{n}(i - \frac{1}{2}) \quad (3)$$

When computing the rainfall of any percentile P, we need to find two consecutive p_k and p_{k+1}, where $p_k < P < p_{k+1}$. The rainfall for this p percentile is therefore

$$r = r_k + \frac{P - p_k}{p_{k+1} - p_k}(r_{k+1} - r_k) \quad (4)$$

Using this approach, we can compute the 25th, 50th and 75th percentile rainfall for each TC category. The analysis results are illustrated by a boxplot (Fig.3) to display the differences between sample populations (McGill et al.[27]). There are five-number summaries for a boxplot: the lower whisker (LW), lower quartile (Q1), median (Q2), upper quartile (Q3), and upper whisker (UW). Q1, Q2 and Q3 are the 25th, 50th and 75th percentile of the population. Points are drawn as outliers if they are larger than Q3+1.5 × (Q3-Q1) or smaller than Q1-1.5 × (Q3-Q1). In Fig.3, two observations are considered as outliers which are depicted by a red plus sign (+). The plotted whisker, UW (or LW) in the figure, is the maximum observation (or minimum observation), which is not an outlier.

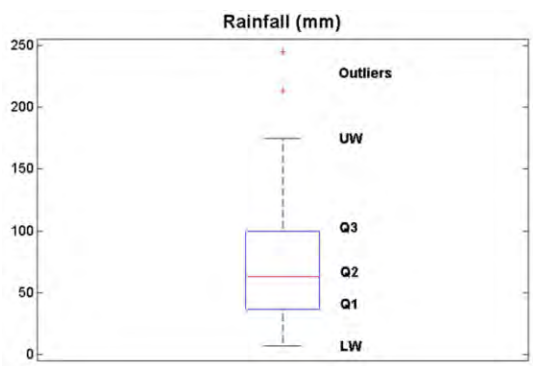

Figure 3. Boxplot as an example.

For practical use of forecasting the rainfall due to a landfalling TC, we first determine the category of the landfalling TC based on the information of TC landfalling distance to SMS from NWP models' forecast and the landfalling intensity from NWP models' forecast, as well as from the empirical experience of the forecasters. Then referring to the boxplot corresponding to the landfalling TC category, we can determine the R-24 and R-72 rainfall at the meteorological station the landfalling TC might cause: the medium rainfall, 25% to 75% interquantile rainfall range, LW, UW, minimum rainfall, and maximum rainfall.

3 STATISTICAL BOXPLOTS FOR TCS RAINFALL

Following the procedures mentioned in section 2, all the historical TCs from 1953-2011 which made landfall within the distance of 700 km to SMS are grouped into 42 categories. Because of the natural selection, it is impossible that each subgroup has approximately equal number of TCs. Table 2 shows the groupings for TCs landfalling on the west of SMS, for example. The 'tms' in the table means the times of TCs for each category. For instance, there are 10 TTYs (2 severe typhoons and 8 typhoons) landfalling on the west of Shenzhen within 100 km distance to SMS (A1-TTY). The 'tms' for other categories are from 4 to 29. For such small sample sizes, nonparametric statistics is seriously suggested to be suitable to analyze the datasets [25]. For each category of the TCs, the minimum, maximum, 25th percentile (Q1), 50th percentile (Q2) and 75th percentile (Q3) of the observed R-24 and R-72 are computed (Table 2).

The boxplots of the historical rainfall records of R-24 and R-72 at SMS due to all the categories of TCs from 1953-2011 are plotted in Fig.4, with a and b for the category TTY; c and d for TTS; e and f for TD. The thick vertical line in each of the sub-plots of Fig.4 refers to SMS. A7, A6, A5, A4, A3, A2, and A1 of the x axis label refer to the TCs landfalling location, which are 600-700 km, 500-600 km, 400-500 km, 300-400 km, 200-300 km, 100-200 km and within 100 km on the west of SMS. respectively. The meanings of B1, B2 ⋯B7 are similar but for the TCs landfalling on the east of SMS. Therefore from Fig.4, we can determine R-24 and R-72 rainfall at SMS that each category of the landfalling TC might cause: the 25% to 75% interquartile rainfall range, the lower whisker (LW), upper whisker (UW), minimum rainfall, and maximum rainfall.

From Fig.4, it can be seen that the shape of the rainfall boxplots is not symmetric comparing the boxplots on the west and on the east of SMS. Generally, the TCs which make landfall on the west of SMS within the distance of 400 km would generally bring more rainfall to SMS than those TCs which make landfall on the east of SMS with similar landfalling intensity and distance. The median (Q2) records for R-24 and R-72 for TTY and TTS (Fig.4a, 4b, 4c, 4d) generally decrease with the increase of the landfalling distance to SMS, especially for TCs landfalling on the west of SMS. However, when the landfalling distance is outside 400 km, Q2 does not decrease as clearly as its change within 400 km. From Fig.4 (a, b, c, d), we can see that TCs which make landfall at B5 (with the distance of 400-500 km on the east of SMS) and B6 (with the distance of 500-600 km on the east of SMS) sometimes

Table 2. Times of each TC category and the corresponding percentile for R−24 and R−72 for TCs landfalling on the west of SMS.

A	R-24 (mm)						R-72 (mm)				
	tms	Min	Max	Q1	Q2	Q3	Min	Max	Q1	Q2	Q3
A1-TTY	10	93.7	247.4	120.3	152.1	226	102.1	347.9	185.8	263.1	290.8
A1-TTS	8	48.2	209.1	93.7	151.1	178.25	111.3	275.7	155	185.95	249.85
A1-TD	6	17.9	121.7	25.8	53.95	89.4	35.9	141.1	45.5	83.75	114.8
A2-TTY	4	101.1	213.5	114.5	140.1	182.9	138.2	478.5	154.1	235.3	389.55
A2-TTS	15	28.3	245.3	36.2	64.6	98.43	34.8	391.6	60.95	93.3	151.38
A2-TD	7	6.6	64.9	33.03	38	55.25	12.3	150.1	52.85	71.2	101.05
A3-TTY	6	23.5	80.9	41.1	60.9	80.3	35.4	131.8	58.5	98.35	114.3
A3-TTS	17	10.7	161	33.9	48.7	65.8	11.7	260	51.08	83.1	143.13
A3-TD	7	10.5	199.7	23.38	35.3	109.25	11.1	282.8	43.85	73.8	145.63
A4-TTY	6	41.9	73.4	54.7	62	68.2	42	128.2	71.3	84.4	90.4
A4-STS	15	4.1	156.6	7.73	36.5	45.95	5.8	261.2	14.7	45.1	96.78
A4-TD	5	15.9	102.5	18.98	22.4	48.2	16.6	105.8	34.08	40.1	65.38
A5-TTY	22	6.1	115	15.4	35.9	54.7	6.7	246.3	24.7	60.05	91.3
A5-TTS	29	0.6	168.8	11.2	26.9	47.5	0.8	189.6	16.58	43.5	74.13
A5-TD	21	1	102	9.1	35.1	46.95	2.4	157.6	13.73	47.4	93.23
A6-TTY	12	0.5	91.4	10.2	22.3	35.1	0.5	140.8	17.3	35.55	48.85
A6-TTS	21	1.4	159.2	6.45	14.7	28.83	1.5	282.5	9.28	24.2	58.73
A6-TD	21	1.1	308.6	6.35	19.2	56.2	1.2	387.8	8.9	31.6	85.78
A7-TTY	10	0.1	45.5	1.9	11.95	21.4	0.1	64.9	2.4	17.55	38
A7-TTS	10	1.2	64.5	6.8	25.85	53.3	1.3	110.1	13.7	52.95	73.7
A7-TD	11	0.1	159.2	1.23	10	33.35	0.1	282.5	2.13	18.3	74.55

might cause very heavy rainfall at SMS. The reason might be that after those TCs land at B5-B6, they do not dissipate soon and continue to move west or east. During their continuing movement, they will probably interact with other weather systems, such as the southwesterly monsoon and mid-latitude trough, and bring plenty moisture and energy to Southeast China. If SMS is on the passageway or near the passageway to transport such moisture and energy, heavy rainfall would occur in Shenzhen. In addition, from Fig.4, it can be seen that the variation of rainfall due to TDs does not change with distance as clearly as rainfall due to other categories of TCs. Furthermore, we can see from the figure that within the distance of 200 km, the median of the rainfall records (Q2) is generally bigger when the strength of the TCs is higher (i.e. $Q2_{TTY}>Q2_{TTS}>Q2_{TD}$). However, when outside 200 km, this pattern might change. For example, rainfall at SMS due to TTSs and TDs which make landfall at B3 is even higher than rainfall due to TTYs landfalling at B3. TTSs which make landfall at B5 (more than 400 km away from SMS) might sometimes induce very large rainfall at SMS (Fig.4c and 4d), as compared to TTYs which make landfall at B5. This might be due to the influence of other factors, such as TC track, TC moving velocity after landfalling and the environmental background etc. How those other TC characteristics and the environmental background influence rainfall intensity and distribution will be analyzed later in a different study.

4 2012, 2013 CASE FORECASTING AND DISCUSSION

To apply the statistical boxplot scheme to forecasting the potential maximum R-24 and R-72 rainfall due to a landfalling TC, we need to first identify the TC landfalling location and intensity. Nowadays operational forecasting models can usually predict the TC track well, especially the track within 24 hours [15]. Compared to the track forecast, the TC intensity forecast by NWP models is not so accurate at present. However, with the real-time observations from satellite and radar, forecasters have the ability to predict the intensity of the landfalling TC 12 hours before TC landfall by rule of thumb, as it usually takes at least 12 hours for a TC to change intensity or motion appreciably [1]. With the approximate TC landfalling location and intensity available 12 hours before the TC landfall, we can then apply the statistical boxplot scheme to forecasting the R-24 and R-72 rainfall at SMS.

In this section, we will use TCs which made landfall along the Southeast China coast in 2012 and 2013 to test the performance of the boxplot scheme. In the typhoon seasons of these two years, there are eleven TCs landfalling within the distance of 700 km to SMS along the Southeast China coast. The detailed TC information is summarized in Table 3.

Based on the latest forecast for these 11 TCs' landfalling direction, location and intensity, the boxplots

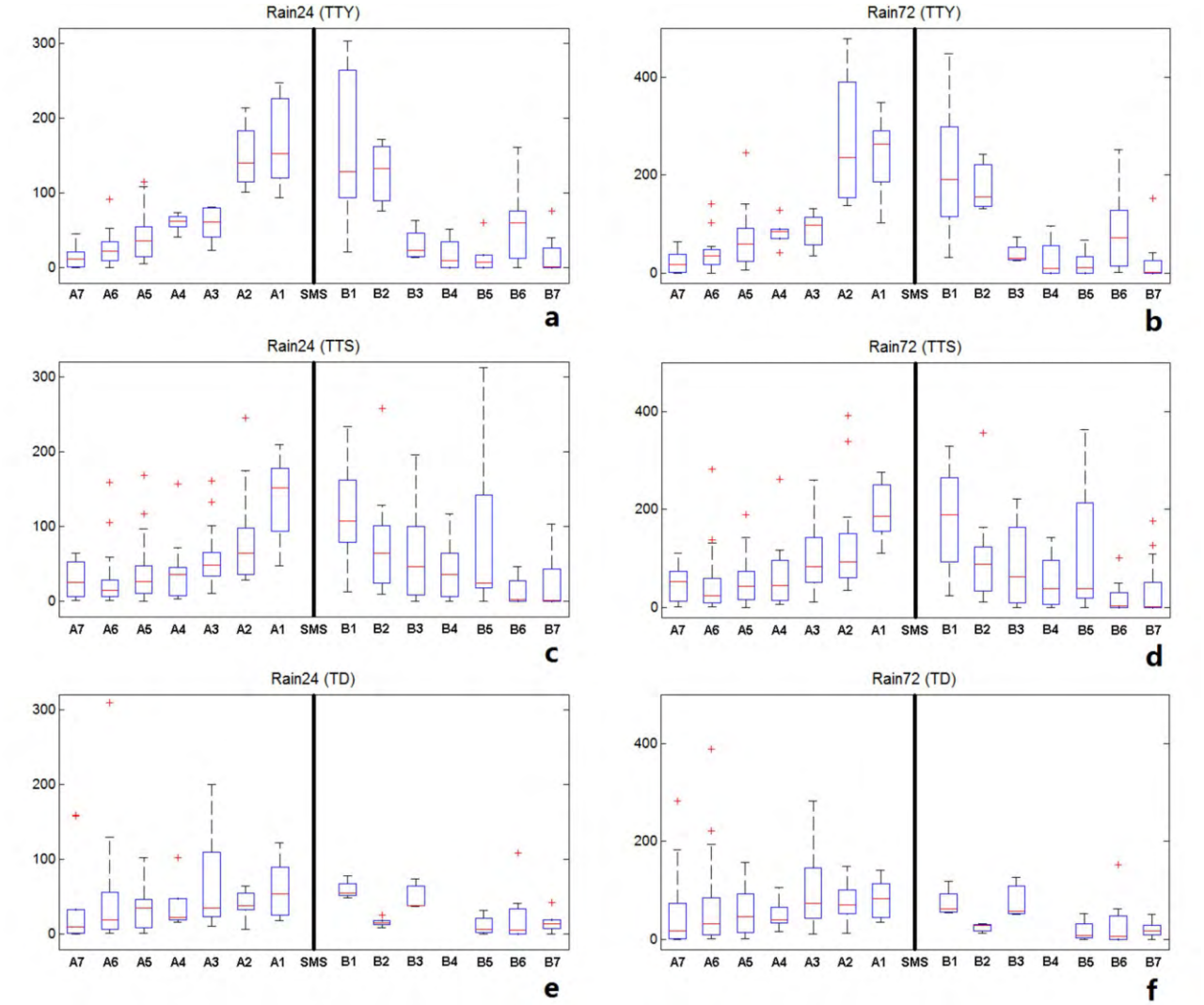

Figure 4. Boxplots for R-24 and R-72 rainfall at SMS from 1953 to 2011 due to TTYs (a and b), TTSs (c and d), and TDs (e and f). The vertical black thick line in the middle of each subplot denotes SMS. "A" on the x-axis refers to the landfalling area, which is to the west of SMS and "B" on the x-axis refers to the landfalling area, which is to the east of SMS. The numbers after A and B refer to the distance to SMS.

Table 3. Information about the eleven TCs landfalling within the distance of 700 km to SMS in 2012 (the first three TCs) and 2013 (the last eight TCs).

Name	Landfalling time	Landfalling Latitude (°N)	Landfalling longitude(°E)	Landfalling intensity	Distance(km)
Doksuri	6/30/0300	22	113.2	TTS	102
Vicente	7/24/0400	22	113	TTY	119
Kai-Tak	8/17/1200	21	110.4	TTY	410
TD1303	6/15/1700	19.9	110.9	TD	436
Bebinca	6/22/1100	19.2	110.7	TTS	506
Rumbia	7/02/0600	21.1	110.2	TTS	424
Cimaron	7/18/2200	24.1	117.9	TTS	434
Jebi	8/02/2000	19.7	110.9	TTS	451
Utor	8/14/1500	21.6	111.9	TTY	241
Trami	8/22/0300	25.7	119.5	TTY	659
Usagi	9/22/2000	22.7	115.4	TTY	263

for the corresponding TC categories are picked out. Fig. 5 shows these boxplots for R-24 rainfall, as well as the real maximum daily rainfall observation at SMS (black and solid horizontal line) during the TC landfalling period (rainfall within a couple of days before and after TC landfalling) due to these TCs. For comparison, the latest rainfall forecasts (brown and solid horizontal line) before the TCs' landfall by European Center for Medi-

um-Range Weather Forecasts (ECMWF) are plotted in Fig.5 as well. ECMWF is renowned worldwide for providing the most accurate medium-range global weather forecasts up to 10 days ahead, monthly forecasts and seasonal outlooks to six months ahead. It has been widely used for operational forecast and research purpose around the world (Xu et al.[28]; Halperin[29]; Wang et al.[30]; Magnusson [31]). ECMWF models are reported to produce well the medium-range forecasts of the Northwest Pacific subtropical high and South Asian high which have pronounced influences on the summertime persistent heavy rainfall in China (Niu and Zhai[32]). The track of the TC in western Pacific and South China Sea is strongly affected by the area of the western Pacific subtropical high (Sun et al.[33]; Tao and Li[34]). Therefore, ECMWF's forecasts of TC's track for the coming 12 and 24 hours are usually reliable. SZMB has been relying on ECMWF for daily operational forecast since 2009. The finest resolution of ECMWF system used in SZMB is $0.125^{o} \times 0.125^{o}$. Xu et al. [28] reported that ECMWF models could provide valuable information for rainfall forecast up to the next 10 days; however, the ability for storm rainfall forecast was not reliable. ECMWF provides medium-range weather forecast twice a day. For TC, ECMWF can usually accurately predict its landfalling intensity change and location by the latest forecast around 12 hours before TC's landfall. Therefore, with the most updated TC intensity observation, as well as the ECMWF forecast, we can obtain the TC's landfalling characteristics 12 hours before its landfall. If the TC makes landfall during 0000-1200 UTC time (universal time), we can obtain the TC's landfalling location and intensity change by referring ECMWF 1200 UTC output of the previous day. Similarly, if the TC makes landfall during 1200-0000 UTC, we could get the TC's characteristic information by referring 0000 UTC ECMWF output of the same day. However, ECMWF cannot predict well the storm rainfall induced by TCs.

From Fig.5, we can see that the observed R-24 rainfall records at SZMB for the 11 TCs are mostly between the historical observed maximum and minimum rainfall for the corresponding category of landfalling TC, except for TY Trami and STY Usagi. TY Trami landed in Fujian province on August 22, 2013. It continued to move west to Jiangxi province, until it finally dissipated in Hunan province. During its process in mainland, Trami interacted with a strong southwest monsoon and brought immense downpours in Southeast China. It set a new rainfall record at Shenzhen for the TTY category which landed on the east of Shenzhen with the landfalling distance of 600-700 km. Similar condition is found for STY Usagi. Usagi set a new rainfall record at Shenzhen for the TTY category which landed on the east of Shenzhen with the landfalling distance of 200-300 km. For the other TCs, most of the rainfall observations at SMS are within the interquartile range of the historical records (Q1 to Q3), such as TS Doksuri, TY Vicente, TY Kai-Tak, TD1303, STS Rumbia, STS Jebi and STY Utor which are shown in Fig.5(a), (b), (c), (d), (f), (h) and (i) respectively. Similarly, more than 50% of R-72 rainfall at SMS due to these TCs is within the interquartile range (Q1 to Q3) of the historical records. By comparison, we can see that the latest ECMWF model output can sometime accurately forecast the rainfall due to TCs, such as in Fig. 5f and 5g. However for the other cases, discrepancies are big between the rainfall forecast by ECMWF and the real rainfall observation at SMS. Therefore besides the NWP, forecasters can use the historical rainfall observation boxplots (Fig.4) as a good reference to predict the potential short-term rainfall due to a landfalling TC.

The statistical boxplots scheme can provide valuable information to operational forecasters to predict the potential rainfall due to a TC. However, we must be aware that there are still a lot of uncertainties for the boxplots because of the small sample size for some TC categories due to the natural features. With more TCs landfalling along the Southeast China coast in future, the database of TCs will be larger and the short-term TC rainfall prediction will be more accurate by the boxplots scheme.

5 CONCLUSIONS

This study applied all the historical TCs landfalling along the Southeast China coast from 1953-2011 to explore a statistical boxplot scheme to forecast the maximum daily (R-24) and three-day accumulative rainfall (R-72) at a certain rain gauge (SMS) during TC landfall. Three TC's characteristics, including TC's landfalling direction, landfalling distance to SMS and landfalling intensity are considered to categorize all the historical TCs landfalling within the distance of 700 km to SMS. The corresponding historical daily rainfall records at SMS during the TC landfalling period (rainfall within a couple of days before and after TC landfalling) are collected and organized according to the TC's category. The organized rainfall records for each TC category are analyzed by percentile estimation. The results are plotted in boxplots. It is concluded from the boxplots that the rainfall at a certain area is generally positively correlated to the intensity of the landfalling TC within the distance of 200 km to the landfalling center. Within the distance of 400 km to the landfalling location, the rainfall at SMS is generally negatively associated with the distance between TC's landfalling center and SMS. With the same intensity scale, TCs landfalling on the west of SMS will generally bring heavier rainfall at SMS than TCs landfalling on the east of SMS within the distance of 400 km. Eleven TCs landfalling within the distance of 700 km to SMS in 2012 and 2013 are used to evaluate the performance of the statistical boxplots in predicting short-term rainfall at SMS. Results show that the boxplot scheme is very valuable to fore-

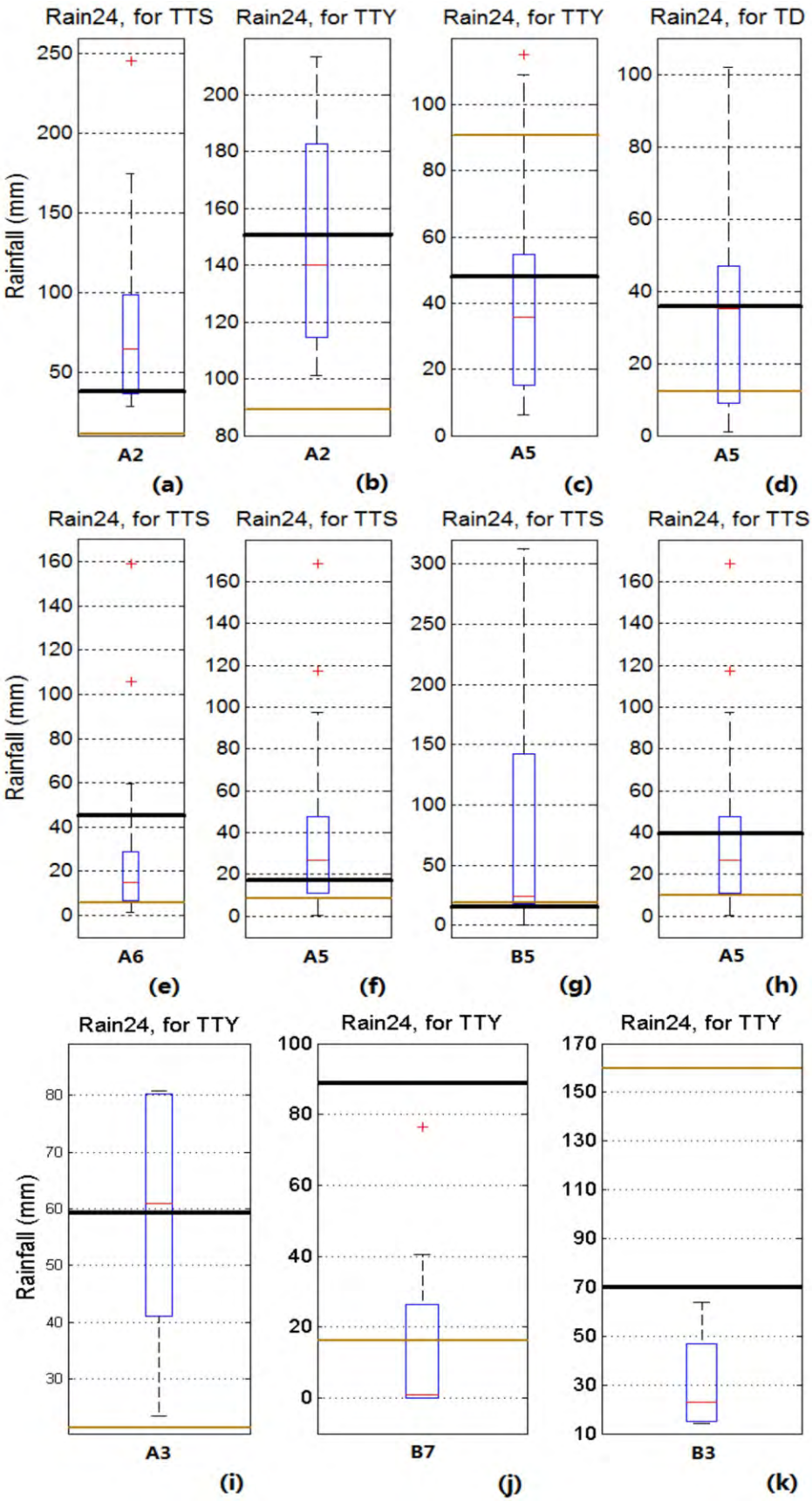

Figure 5. Comparison of the R-24 rainfall forecasts for 11 TC cases in 2012 and 2013 by the boxplots and by ECMWF (brown solid horizontal line), as well as the real rainfall observation (black thick solid horizontal line): (a) for TS Doksuri; (b) for TY Vicente; (c) for TY Kai-Tak; (d) for TD1303; (e) for TS Bebinca; (f) for STS Rumbia; (g) for STS Cimaron; (h) for STS Jebi; (i) for STY Utor; (j) for TY Trami and (k) for STY Usagi.

casters to provide rainfall range for each TC category. For most of the time, the observed rainfall due to a landfalling TC is within the range of the historical rainfall records.

The boxplot scheme is easy to implement. The rainfall boxplots are quite helpful to operational forecasters. As of this writing, the technique is already in use as a valuable reference at SZMB to predict the short-term rainfall at SMS due to TCs.

REFERENCES:

[1] WILLOUGHBY H E, RAPPAPORT E N, MARKS F D. Hurricane Forecasting: The State of the Art [J]. Nat Haz Rev, 2007, 8(3): 45-49.

[2] WU L, LIANG J, WU C. Monsoonal influence on Typhoon Morakot (2009). Part I: observational analysis [J]. J Atmos Sci, 2011, 68: 2 208-2 221.

[3] JONKMAN S, MAASKANT B, BOYD E, et al. Loss of life caused by the flooding of New Orleans after Hurricane Katrina: A preliminary analysis of the relationship between flood characteristics and mortality [C]// 4th International Symposium on Flood Defence, Managing Flood Risk, Reliability and Vulnerability. Toronto, Ontario, Canada, Institute for Catastrophic Loss Reduction, 2008, (96)1-9.

[4] CUI Peng, CHEN Su-chin, SU Feng-huang et al. Formation and Mitigation Countermeasure of Geo-hazards Caused by Morakot Typhoon in Taiwan [J]. J Mount Sci, 2010, 28(1): 103-115 (in Chinese).

[5] KNABB R D, RHOME J R, BROWN D P. Tropical Cyclone Report: Hurricane Katrina: 23-30 August 2005 [EB]. http://www.nhc.noaa.gov/pdf/TCR-AL122005_Katrina.pdf, (December 20, 2005; updated August 10, 2006; Updated September 14, 2011), available Nov.1, 2013.

[6] KIDDER S Q, KUSSELSON S J, KNAFF J A, et al. The Tropical Rainfall Potential (TRaP) technique. Part I: description and examples [J]. Wea Forecast, 2005, 20(4): 456-464.

[7] ABERSON S D. The ensemble of tropical cyclone track forecasting models in the North Atlantic basin (1976-2000) [J]. Bull Amer Meteorol Soc, 2001, 82(9): 1 895-1 904.

[8] FEI Jian-fang, LI Bo, HUANG Xiao-gang et al. On the relationships between the unusual track of typhoon Morakot (0908) and the upper westerly trough [J]. J Trop Meteorol, 2012, 18(2): 187-194.

[9] ROGERS R, ABERSON S, BLACK M, et al. The Intensity Forecasting Experiment: A NOAA Multiyear Field Program for Improving Tropical Cyclone Intensity Forecasts [J]. Bull Amer Meteorol Soc, 2006, 87(11): 1 523-1 537.

[10] DEMARIA M, GROSS J M. Chapter 4: Evolution of Tropical Cyclone Forecast Models [M]// Hurricane! Coping with Disaster, Robert Simpson, American Geophysical Union, 2003, ISBN 0-87590-297-9, 360 pp.

[11] CECIL D J, JONES T A, KNAFF J A, et al. Statistical forecasting of Pacific and Indian Ocean tropical cyclone intensity using 19-, 37-, and 85- GHZ brightness temperatures [C]// 26th Conference on Hurricanes and Tropical Meteorology, Miami: Amer Meteorol Soc, 2004, 302-303.

[12] KNAFF J A, SAMPSON C R, DEMARIA M. An operational statistical typhoon intensity prediction scheme for the western North Pacific [J]. Wea Forecast, 2005, 20(4): 688-699.

[13] MARCHOK T, ROGERS R, TULEYA R. Validation Schemes for tropical cyclone quantitative precipitation forecasts: Evaluation of operational models for U.S. landfalling cases [J]. Wea Forecast, 2007, 22(4): 726-746.

[14] LIU G, CHAO C, HO C. Applying satellite-estimated storm rotation speed to improve typhoon rainfall potential technique [J]. Wea Forecast, 2008, 23(2): 259-269.

[15] XU Ying-long, ZHANG Ling, GAO Shuan-zhu. The advances and discussions on China operational typhoon forecasting [J]. Meteorol Mon, 2010, 36 (7): 43-49 (in Chinese).

[16] CHEN Lian-shou. Research progress on the structure and intensity change for the landfalling tropical cyclones [J]. J Trop Meteorol, 2012, 18(2): 113-118.

[17] SIMPSON R H, RIEHL H. The Hurricane and Its Impact [M]. Louisiana State University Press, 1981, 398 pp.

[18] PFOST R L. Operational tropical cyclone quantitative precipitation forecasting [J]. Nat Wea Dig, 2000, 24(1-2): 61-66.

[19] CHAN J C L, LIANG X. Convective asymmetries associated with tropical cyclone landfall. Part I: f-plane simulation [J]. J. Atmos. Sci., 2003, 60(13): 1 560-1 576.

[20] WANG Ming-jie, ZHANG Xiao-li, LI Xing-rong. Analysis of meteorological conditions for the base of marine sports in the 26th Summer Universiade in Shenzhen in 2011 [J]. J Trop Meteorol, 2011, 17(2): 187-192.

[21] ZHANG Xiao-li, LI Lei, DU Yan, et al. A numerical study on the influences of urban planning and construction on the summer urban heat island in the metropolis of Shenzhen [J]. J Trop Meteorol, 2011, 17(4): 392-398.

[22] CHEN J, LI Q, NIU J et al. Regional climate change and local urbanization effects on weather variables in southeast China [J]. Stoch Environ Res Risk Assess, 2011, 25 (4): 555-565, doi: 10.1007/s00477

[23] LI Q, CHEN J. Teleconnection between ENSO and climate in South China [J]. Stoch Environ Res Risk Assess, 2014, 28(4): 927-941, doi:10.1007/s00477-013-0793-z

[24] TURCO M, LLASAT M C. Trends in indices of daily precipitation extreme in Catalonia (NE Spain), 1951-2003 [J]. Nat Haz Earth Syst Sci, 2011, 11: 3 213-3 226.

[25] PETT M A. Nonparametric statistics for health care research-Statistics for small samples and unusual distributions [M]. Sage Publications, Thousand Oaks, 1997.

[26] STARK H, WOODS J. Probability, Statistics, and Random Processes for Engineers (4th Edition) [M]. Pearson, Boston, 2012.

[27] MCGILL R, TUKEY J W, LARSEN W A. Variations of Box Plots [J]. J Amer Stat Assoc, 1978, 32(1): 12-16.

[28] XU Wen-wen, CHEN Shen-peng, LI Qing-lan, et al. Evaluation of precipitation forecast in Shenzhen for the first raining season in 2012 by ECMWF model and HAPS model [J]. Guangdong Meteorol, 2013, 35(5): 6-9 (in Chinese).

[29] HALPERIN D J, FUELBERG H E, HART R E, et al. An evaluation of tropical cyclone genesis forecasts from global numerical models [J]. Wea Forecast, 2013, 28(6): 1 423-1 445.

[30] WANG Y, BELLUS M, GELEYN J F, et al. A new method for generating initial condition perturbations in a regional ensemble prediction system: Blending [J]. Mon Wea Rev, 2014, 142(5): 2 043-2 059.

[31] MAGNUSSON L, BIDLOT J R, LANG S et al. Evaluation of medium-range forecasts for hurricane Sandy [J]. Mon Wea Rev, 2014, 142(5): 1 962-1 981
[32] NIU Ruo-yun, ZHAI Pan-mao. Synoptic verification of medium-extended-range forecasts of the northwest Pacific subtropical high and South Asian high based on multi-center TIGGE data [J]. Acta Meteorol Sinica, 2013, 27 (5): 725-741
[33] SUN Y, ZHONG Z, LU W et al. Why are tropical cyclone tracks over the western North Pacific sensitive to the cumulus parameterization scheme in regional climate modeling? A case study for Megi (2010) [J]. Mon Wea Rev, 2014, 142(3): 1 240-1 249.
[34] TAO Li, LI Shuang-jun. Impact of tropical intraseasonal oscillation on the tracks of tropical cyclones in the western North Pacific [J]. J Trop Meteorol, 2014, 20 (1): 26-34.

Citation: LI Qing–lan, LAN Hong–ping, Johnny C L CHAN, et al. An operational statistical scheme for tropical cyclone induced rainfall forecast [J]. J Trop Meteorol, 2015, 21(2): 101–110.